International Journal of Power and Energy Systems, Vol. 42, No. 10, 2022
An Open Access Paper

STRUCTURAL ANALYSIS OF 420 kV POLYMER-HOUSED SURGE ARRESTER

Konthedath M.M. Muneer,* Neelam Tiwari,* Supak Pore,* Manish C. Gupta,* and Mandava M. Rao*

Abstract

The present paper discusses about the structural analysis of polymer-housed surge arrester (SA) along with its support structure for ultra-high voltage applications. The main objective of the work is to study the effect of various geometric parameters on the static and dynamic responses of the SA assembly and hence to finalize the mechanical design of the integrated equipment–structure combination. As it is cumbersome to generate detailed finite element model and conduct iterative analysis manually, an automation tool has been developed in ANSYS using ANSYS Parametric Design Language (APDL) to ease numerical modelling and structural analysis. Here, the input parameters are entered through a user interface developed in VB.Net. Sensitivity analyses have been conducted to compute the effect of various parameters on the static and dynamic responses of the polymer-housed SA assembly. The analyses results indicate that cantilever deflection of polymer-housed SA is most sensitive to thickness variation of flange followed by insulator tube thickness and elastic modulus of a tube material made of fibre-reinforced polymer. A 420 kV SA assembly finalized based on structural responses is further analysed to compute voltage distribution across metal oxide blocks and electrostatic field across polymer housing.

Key Words

Substation, surge arrester, polymer housing, composite insulator, finite element method, natural frequency, modal analysis, response spectrum

1. Introduction

The layout of the air-insulated switchgear (AIS) consists of parts such as circuit breakers, isolators, earthing switch, current and voltage transformers, and surge arresters (SAs). These substations experience lightning, switching and temporary overvoltages during service. SA is one of the important modules of high voltage (HV) substation that helps to prevent damage to electrical apparatus due to HVs generated by switching or lightning. The arrester provides a low-impedance path to ground for the current from a lightning strike or transient voltage and then restores to normal operating conditions [1]. When an HV due to lightning strikes on the transmission line, the arrester instantly furnishes a conducting path to ground and thus limits the excess voltage. The arrester provides relief against overvoltages and prevents further flow of current to the ground.

In AIS, the SAs are primarily installed at the line entrances and as a complementary protection at strategic points of the substation, often at the transformers. Due to relatively higher surge impedance of the AIS elements, the arrester gives a limited protection length. In general, SA assembly consists of multiple SA stacks, support structure, grading shield, HV conductor, clamps, *etc.* Height of the SA depends on its rated voltage, and number of columns depends on current discharge capability. Higher voltage equipment tends to be more vulnerable due to the larger electrical clearances from the ground or between phases, leading to increased height of insulators. The tall structures and apparatus may result to large amplification of input motions because of their flexibility [2]. Thus, structural integrity of the equipment in the substation is very important as they are exposed to natural phenomena like wind and seismic events.

In electrical substation, insulators act as load-carrying structure for most of the power equipment. However, its heavy mass and brittle nature result in poor structural performance especially during tensile loads [3]. In ultra-high voltage (UHV) substations, relatively taller equipment is designed for higher electrical clearances which in turn require better mechanical strength. Consequently, structural safety of UHV substation becomes more challenging. Thus, composite insulators, as shown in Fig. 1, made of fibre-reinforced polymer (FRP) with silicon sheds become alternative for such applications as they improve the structural performance of the equipment [3], [4]. It is also noted that polymer-housed arresters with hydrophobic materials like silicone rubber have a better pollution performance compared to porcelain due to reduced leakage currents.

Dynamic properties of equipment–support system were studied using parametric models [5]. Using a four degrees of freedom (DOF) model for equipment–support system, a new equation was proposed to calculate natural frequency of different equipment–support combinations. Based on the dynamic amplification studies, minimum stiffness ratio required for equipment–support combination was also pro-

* Bharat Heavy Electricals Limited (BHEL), Corporate R&D, Hyderabad, India; e-mail: {muneerkm, neelamtiwari, supakpore, manishg, mmrao}@bhel.in
Corresponding author: Mandava M. Rao
Recommended by Dr. Zakir Rather
(DOI: 10.2316/J.2022.203-0385)

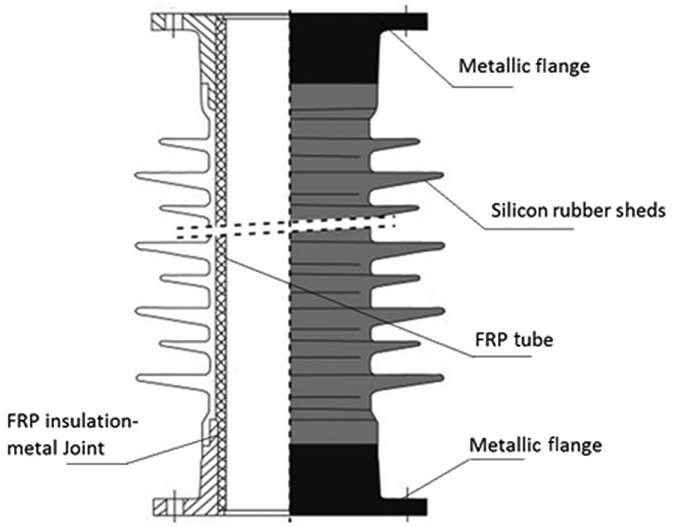

Figure 1. Section of polymer housing with silicon rubber sheds.

posed so as to keep dynamic amplification factor (DAF) to be smaller than the target DAF as per IEEE-693 [6]. Few authors conducted experimental study on 230 kV disconnector switches made of porcelain and composite insulators [7]. It was found that despite having lighter mass than the porcelain insulators, the polymer insulators are more favourable from a seismic performance perspective. A shaking table test on a 230 kV disconnector switch with support structure was conducted, and displacement responses of the equipment mounted on supporting frames with different flexibility were studied through numerical analysis [8].

Investigation on the interaction effects of SA and support structure during seismic excitation found that bending moment at the base and displacement at the top of the equipment are the critical factors. It was also concluded that seismic responses of the system are dominated by the dynamic responses of first mode [3]. Few authors also studied the effect of sheds and cemented joint between insulator and metal cap on dynamic properties of porcelain equipment during seismic events. The effect of sheds and cemented joint were considered in seismic modelling and equations were derived for estimating flexural stiffness at the interface [9]. Few researchers investigated to improve the seismic performance of 800 kV wall bushing of valve hall system by developing finite element (FE) model [10]. Further, seismic qualification test was conducted on 132 kV SA along with support structure [11] and concluded from the dynamic responses that the system was "seismically qualified" as no stiffness degradation was observed. In service conditions, the equipment is also subjected to other loads such as jumper/HV conductor and wind loads, and it needs to be qualified for these lateral loads. In the literature, it is hard to find any studies giving due importance to structural responses against these loads along with seismic effects. In view of the above, the present paper investigates the effect of various geometric parameters of equipment on static and dynamic responses due to these design loads.

2. Development of Automation Tool for Numerical Modelling

In AIS SAs, the non-linear metal oxide (MO) blocks stacked in series and connected by metallic element are placed in an insulating FRP tube of high mechanical and dielectric strength. The metallic element or contact plate is designed with a suitable profile to control E-field in the vicinity, and insulating tube is terminated with metallic flanges. The SA assembly is connected with other equipment electrically by means of flexible or rigid conductors at the top. The flexible conductor is set with slackness and the rigid bus is assembled with a sliding slot for necessary expansion/contraction. Higher displacement at the top of SA may result in excessive interaction among nearby equipment, which leads to huge induced forces. As the paper is intended to evaluate the effect of various parameters on static and dynamic responses of SA with supporting structure, it is necessary to analyse a huge number of equipment–support combinations. This makes it difficult to generate detailed FE models on case-to-case basis. Hence to ease the study, developing a parametric model is the most appropriate. Accordingly, numerical modelling has been automated in the ANSYS APDL platform with user interface using VB.Net (refer Fig. 2). The primary objective of the present study is to determine the structural parameters of the polymer-housed SA, satisfying both static and dynamic considerations as per relevant indian standards (IS) and international electrotechnical commission (IEC) standards. The tool is designed in such a way that geometric inputs are entered through a graphical user interface (GUI), which generates APDL-based macros for all modules (Fig. 2), *i.e.*, "MODEL", "STATIC ANALYSIS" and "DYNAMIC ANALYSIS" in ".mac" format, wherein numerical modelling, loading and finally static and dynamic analyses are conducted. The macros are then executed in the ANSYS platform utilizing its in-built capability. Overall, data flow is captured in the flow diagram (Fig. 3) with input parameters entered through GUI, and chronological order of processes is depicted.

3. Finite Element Modelling

The most preferred numerical method to simulate an electrical equipment and its supporting structure is FE technique [5]. The mechanical properties of the materials considered for the components in the numerical modelling are presented in Table 1. The damping ratio of these equipment is assumed to be 2% as per IEEE recommendations. It is the best practice to model the equipment by considering its in-service configuration. Thus, the numerical model of integrated SA with the support structure is developed in ANSYS 17.0. The geometry and thickness of each component are obtained through the electro-mechanical design of the insulator. Composite insulator, flanges and supporting plates are modelled as shell elements using four-node SHELL63 [12] element which has both bending and membrane capabilities. The supporting structure of SA is modelled using a linear, two-node BEAM188 [12] element, suitable for modelling slender structure. Both the elements

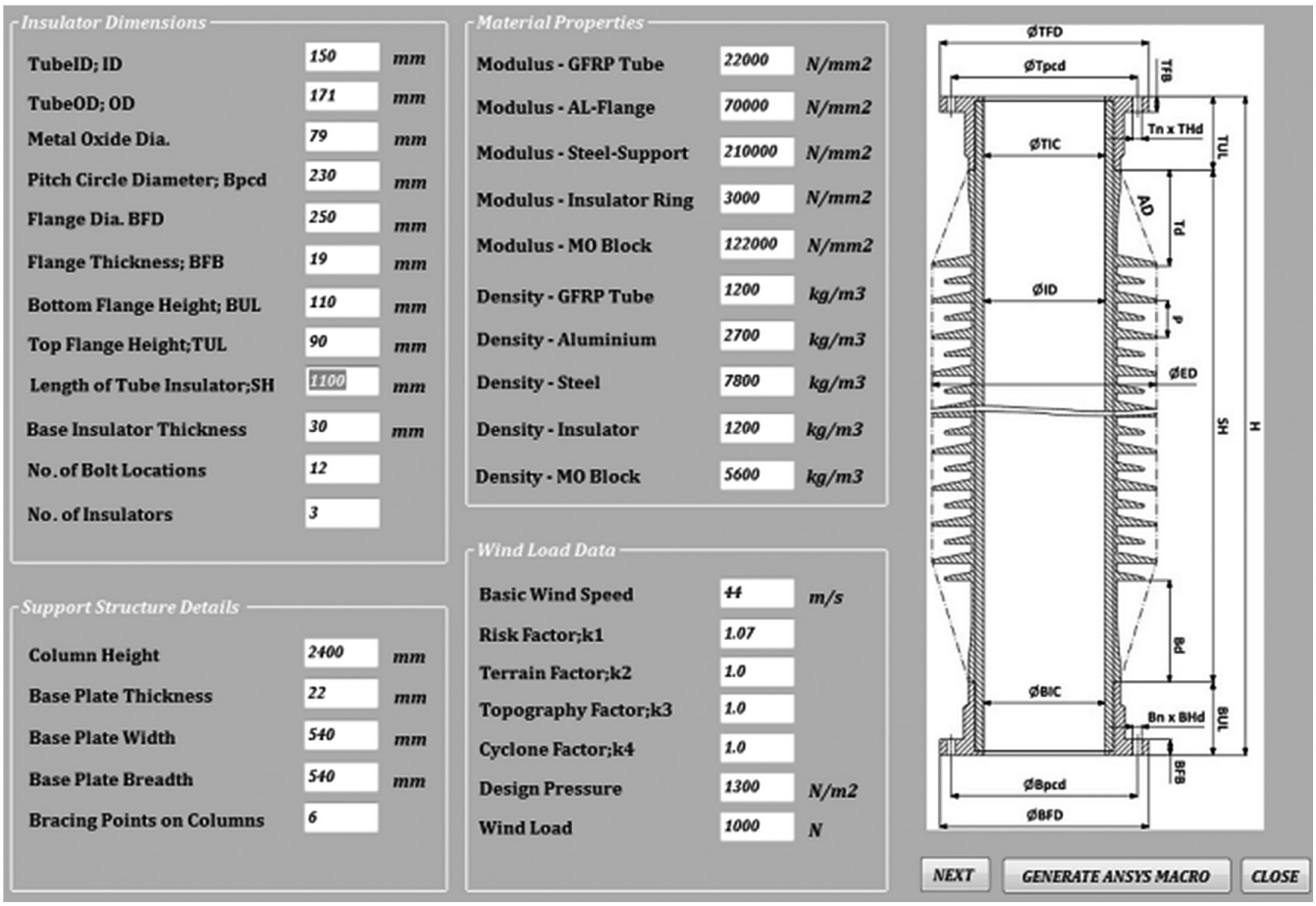

Figure 2. User interface for geometric input.

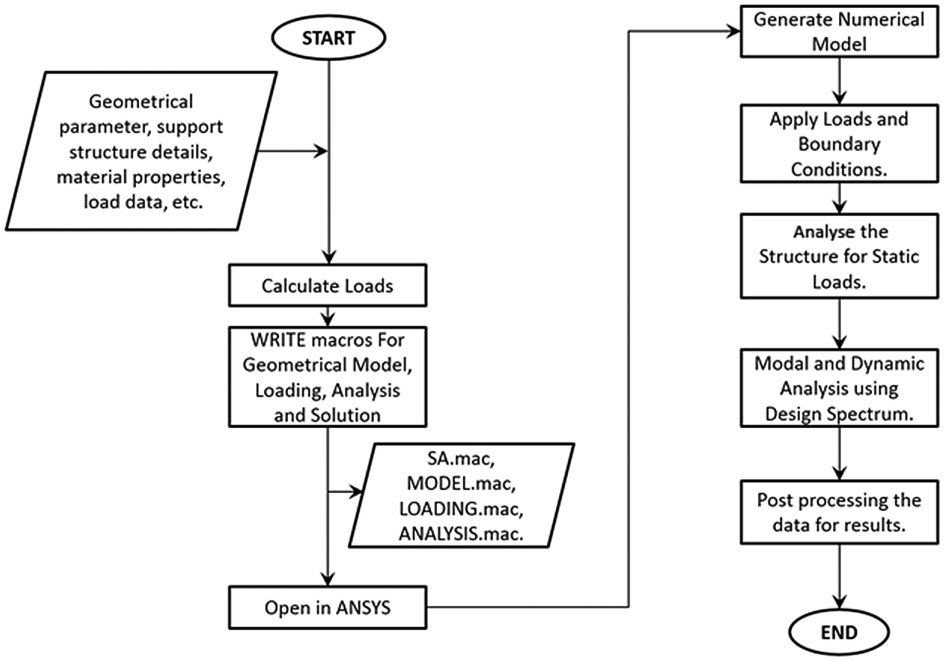

Figure 3. Data flow for automating numerical modelling.

are characterized by six DOF (translations in the nodal x, y and z directions and rotations about the nodal x, y and z-axes) at each node. ZnO blocks along with the contact plate/metal spacer are considered as continuous beam inside the composite insulator and are modelled as beam elements with circular solid section. Precisely, spring-loaded

Table 1
Mechanical Properties of the Materials

Material	E (GPa)	μ	ρ (kg/m^3)
Steel	210	0.3	7,800
Aluminium	70	0.33	2,700
FRP	22	0.22	1,200
ZnO block	122	0.35	5,600

E: Young's modulus, μ: Poisson's ratio, ρ: Density.

blocks of ZnO along with closely packed anti-skid discs are considered as a single unit which would be assisting the insulator tube in increasing flexural rigidity and modelled as beam elements. Section attributes and orientation of beam sections are taken care at definition stage itself. Connectivity between the flanges of stacked insulators has been provided by coupling nodes at their interface. The bolted connection between the structure assembly and foundation is modelled as moment-free constraints. Mass of internals and other non-structural members are accounted by adjusting the density of modelled components. The thickness of silicone sheds is small when compared to that of composite insulator core; hence, effect of sheds is less significant [9].

4. Methodology of Load Estimation

SA is an important module of substation equipment which has slender shape. The polymer insulators act as main load-carrying structure. The polymer insulator transfers dead weights of top connectors, grading ring at the top, MO blocks and aluminium flanges in the axial direction of the insulator tube. Lateral loads, such as wind and seismic effects of electrical equipment, are transferred through bending, wherein flexural rigidity of composite insulator is more important [13]. Apart from these, another important one is the shock load on the insulator due to the sudden loss of strength in the interconnected equipment during mechanical failure.

4.1 Jumper Load

Electrical equipment is connected to each other in HV substation to form necessary configuration [14]. Loosing strength of any equipment shall cause a significant load increase in nearby equipment. When mechanical load of equipment is suddenly thrown, rocking would happen to slender equipment. As the equipment is connected with each other by rigid bus bars with a sliding slot or flexible conductor with slackness, the rocking of equipment may cause shock load to nearby equipment [13]. The impulsive load in the lateral direction is considered as jumper load.

4.2 Wind Load (IS 875: Part 3)

Wind action is evaluated by the pressures or by the forces. The effect of wind on structures is depending on wind properties and structure characteristics. The wind velocity is dependent upon the geographic region, terrain category, shielding and the topographic location of a building site, whereas the wind pressure coefficients are dependent upon the equipment geometry. The design wind speed (V_z) is determined from basic wind speed [15]:

$$V_{\mathrm{z}} = V_{\mathrm{b}} * k_1 k_2 k_3 k_4 \tag{1}$$

where V_{b} is the basic wind speed, k_1 is the risk factor, k_2 is the terrain, height and structure size factor, k_3 is the topography factor and k_4 is the importance factor for cyclonic region.

Wind pressure acting on the equipment surface is obtained from the following equation:

$$P_{\mathrm{z}} = 0.5\rho * V_{\mathrm{z}}^2 \tag{2}$$

where ρ is the mass density of air. The recommended value for ρ is 1.25 kg/m^3 (at sea level and 20 °C). The pressure forces acting normal to the structural elements can be calculated from the following equation:

$$F_{\mathrm{memb}} = C_f A P_z \tag{3}$$

where F_{memb} is the wind forces acting on the structural members. C_f is the force coefficient for individual structural members of infinite length and A is the projected surface area of the FRP insulator.

4.3 Seismic Load: The Response Spectrum Method (IS 1893–2002)

Response spectrum is the most widely used method in the seismic analysis. It can be performed using the design spectrum shown in Fig. 4 or a site-specific design spectrum. The dynamic response of the system is represented by the lateral displacements of the lumped masses with the number of degrees of dynamic freedom (or modes of vibration "n") being equal to the number of masses. When the ground motion is applied to the base of the multi-mass system, the deflected shape of the system is the combination of all mode shapes, which can be obtained by the superposition of the vibrations of each lumped mass. Each individual mode of vibration of a multi-mass system has

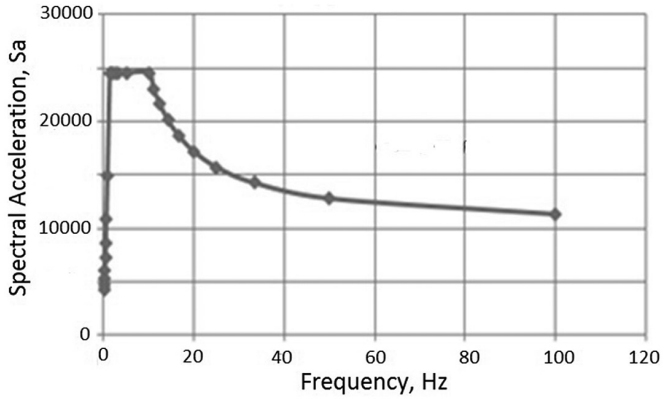

Figure 4. Response spectra for rock and soil sites for 5% damping [16].

Table 2
Seismic Parameters

Item	Description	Value
I	Importance factor	1.75
R	Reduction factor	4
Z	Zone factor	0.36

its own period of vibration and a unique mode shape. Each predominant mode is analysed separately, and the results are combined statistically to obtain the total response (methods such as square-root-of-the squares or the complete quadratic combination method). As IS 1893 [16] recommended, highest possible number of modes to be included in the analysis to ensure that at least 90% of the total seismic mass is excited by them. For the purpose of determining seismic forces, the country is divided into four seismic zones, II, III, IV and V. The horizontal seismic coefficient Ah for a structure is determined by the following equation [16]:

$$A_{\mathrm{h}} = \frac{ZI}{2R}\left(\frac{S_{\mathrm{a}}}{g}\right) \tag{4}$$

And design seismic base shear, V_B, can be determined by the following equation [16]:

$$V_{\mathrm{B}} = A_{\mathrm{h}} W \tag{5}$$

where Z is the zone factor, I is the importance factor, R is the response reduction factor, S_a/g is the average response acceleration and W is the seismic weight of the structure. Figure 4 shows the proposed 5% spectra for rocky and soil sites. In the present paper, it is proposed to qualify the structure for the most severe seismic activity at soft soil site, accordingly parameters have been chosen for the analysis and listed in Table 2.

5. Results and Discussion: Structural Analysis

Numerical model of SA assembly developed in ANSYS has been analysed with appropriate boundary conditions at the supports. Jumper load, wind load in both directions and seismic load are considered as primary loads. Jumper load is applied at the tip of the insulator in the horizontal direction, whereas wind load is applied all over the structure as uniformly distributed load. Loading parameters are specified in Table 3. Cantilever deflection of the insulator is expected to be critical, which needs to be addressed while finalizing the geometric parameters. Now, as the SA is connected with other equipment by the flexible conductor or rigid bus/conductor at the top, the displacement needs to be controlled within allowable limits. If it is more than the slackness of the conductor or the length of sliding slot, excessive interactive forces may be induced on nearby equipment. In fact, the elevated loading can be avoided by increasing the slackness of the flexible conductor or sliding length of the joint. However, increasing slackness of the flexible conductor causes stronger oscillation of the

Table 3
Jumper and Wind Load Parameters

Item	Value	Unit
Jumper load	200	kgf
Basic wind speed	44	m/s
Risk factor, k_1	1.06	–
Terrain factor, k_2	1.05	–
Topography factor, k_3	1.0	–
Cyclonic factor, k_4	1.0	–

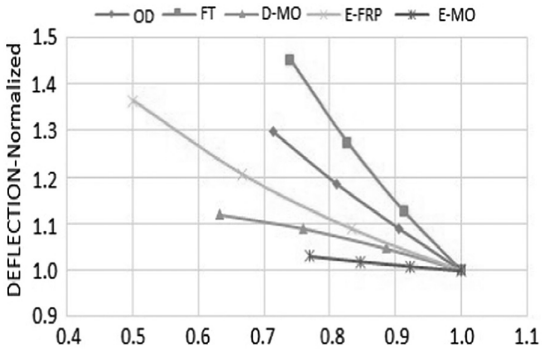

Figure 5. Sensitivity of various parameters on cantilever deflection.

conductor under wind load, and it is also necessary to increase the height of equipment or support to maintain safety clearance between the flexible conductor and the ground. For rigid bus, increasing the sliding length may lead to assembly-related problems.

Hence, it is certain that the displacement demand of the equipment should be limited to avoid undesirable interaction between equipment [3]. Thus, from the above discussions, it is apparent that flexural rigidity is the most important parameter to control structural response during such lateral loading conditions. It is also important to understand the impact of various geometric parameters on cantilever deflection. Hence, iterative analyses were conducted to determine static and dynamic responses of the insulator with various combinations of geometric parameters. Sensitivity of a set of selected parameters such as insulator tube thickness (OD), aluminium alloy flange thickness (FT), diameter of metal oxide (D-MO) block, elastic moduli of FRP tube (E-FRP) and elastic moduli of metal oxide (E-MO) block on cantilever deflection is studied and presented in Fig. 5. It can be observed from the analysis results that the insulator deflection is most sensitive to the thickness variation of flange (FT) followed by insulator tube thickness (OD) and elastic modulus of FRP tube (E-FRP). So, practically for higher stiffness, it may be more convenient to alter flange thickness rather than modifying insulating tube dimensions or properties. Deflected shape of the composite insulator during jumper load in X-direction and wind load in Z-direction is shown in Fig. 6. Jumper load induces 35.8 mm deflection at the

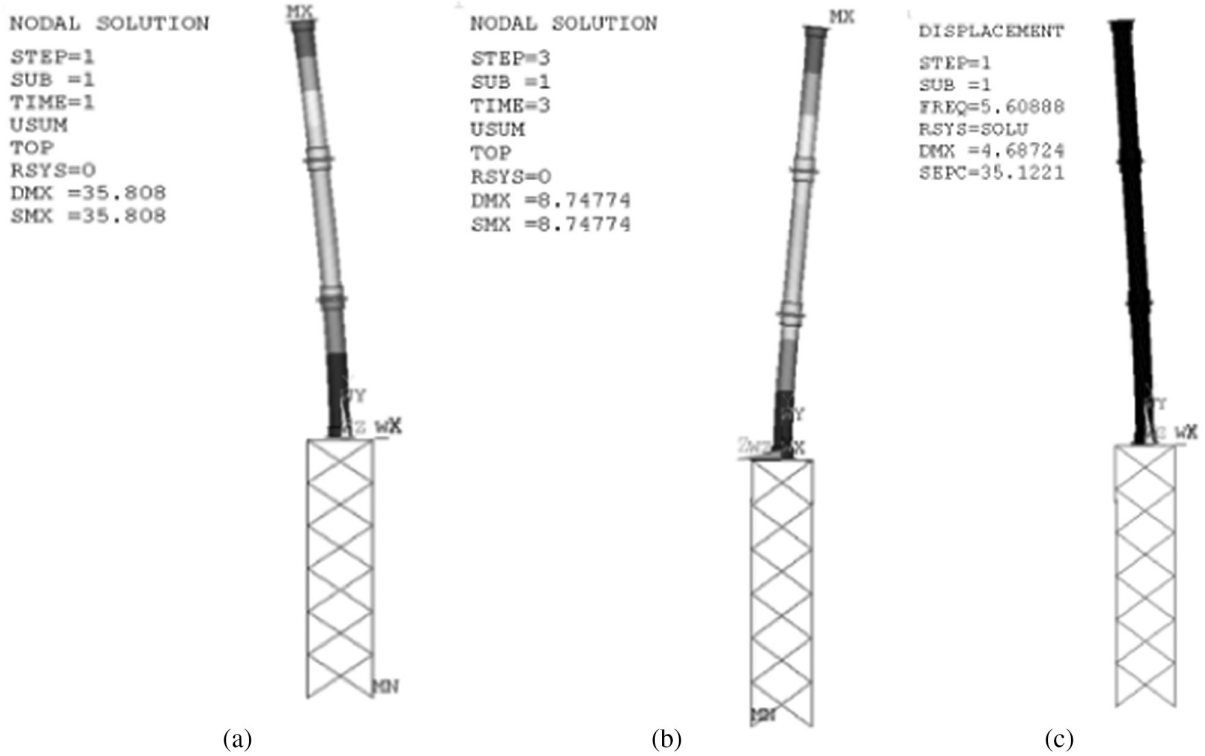

Figure 6. Structural responses during (a) jumper load, (b) wind load and (c) first mode frequency.

tip, and the maximum deflection caused by wind load is 8.75 mm. The MO block-stacked composite insulator is connected to support structure (steel) through a bottom plate of thickness of 22 mm. As expected during jumper and wind loading conditions, the stress developed is maximum at the bottom flange of the insulator viz., 52 and 17.2 MPa, respectively, and are well within the allowable limit.

6. Results and Discussion: Voltage Distribution Analysis

The voltage distribution across SA is highly non-uniform due to the effect of various parameters such as height of arrester, stray capacitance of MO blocks and stray capacitance of metallic flanges. The presence of stray capacitance affects the behaviour of MO SA during both conductive and non-conductive modes of operation. Stray capacitance between arrester blocks and ground plane and compensating capacitance between arrester blocks and HV grading shield modify the voltage distribution across the blocks. Thus, it is essential to compensate the stray capacitance for better voltage distribution, to reduce non-uniformity voltage factor as well as to improve the response time of the SA [17]. To achieve non-uniformity voltage factor within $\pm 10\%$, special grading shields are required. Generally, these shields are provided at HV side of the arrester. The deviation of MO block voltage from its rated voltage increases with the increase in arrester height. Hence, for higher system voltages, design of SAs becomes more complex as compared to lower system voltages. The function of grading ring is also to ensure that the E-field surrounding the arrester is as uniform as possible and less than the allowable limit. In addition to the above, for system voltages of 420 kV and more, it is required to use multiple metallic rings at floating potential to limit corona around metallic flanges of SA column and from metal–insulator interface of the polymer insulator. These additional shields increase the stray capacitance to ground and enhance non-uniformity voltage factor further. To design HV grading shield of SA, a numerical model using ELECTRA software is developed. The air (N_2)-insulated SA model consists of composite insulator housing to keep MO blocks, grading shields and support structure to support the SA (refer Fig. 7(a)). Table 4 shows the input parameters of the 420 kV AIS SA model. To calculate voltage distribution across SA blocks, the HT conductor is energized with rated voltage of 390 kV. Prior to analyse the SA model for voltage distribution, E-field analysis has been carried out on the model to optimize the configuration of the grading shield including its height and diameter. The E-field analysis has been carried out on the model without MO blocks at the basic insulation level, *i.e.*, at 1,425 kV as per IEC 62271-203. Electric field distribution around grading ring and other metal flanges are calculated (refer Fig. 7(b)) and maintained to be less than the allowable levels. To ensure discharge-free system during service, the electric field along the polymer insulating surface is calculated (Fig. 7(c)) and maintained much less than air ionization levels. To understand the effect of grading shield design on non-uniformity factor, the voltage distribution across blocks has been calculated for the proposed model with and without shield (refer Fig. 8). From Fig. 8, it is evident that the overvoltage factor is about 102% on the MO block near the HV terminal. By employing HV grading shield of diameter 1,200

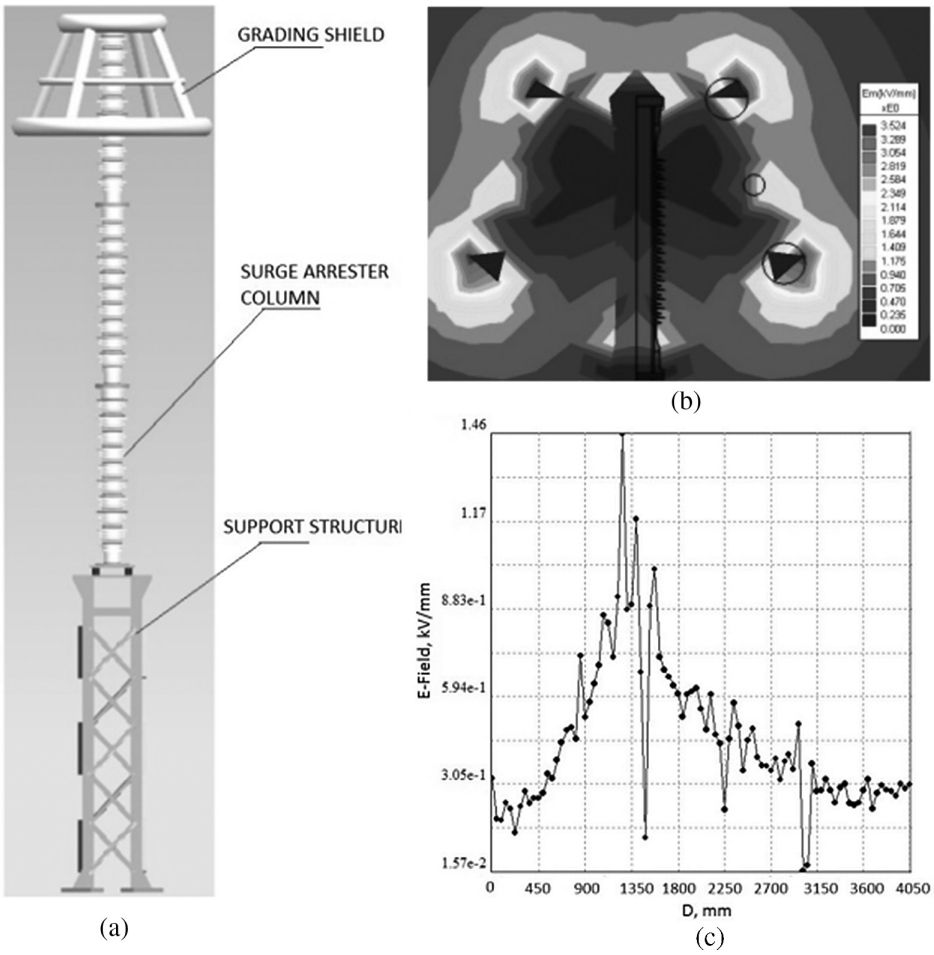

Figure 7. 420 kV AIS surge arrester: (a) SA model, (b) E-field around grading shield and (c) E-field along polymer insulator surface.

Table 4
Input Parameters of 420 kV SA Model

Parameters	Value
System voltage in kV	420
Rated voltage in kV	390
Basic insulation level, kVp	1,425
Capacitance of ZnO block, pF	750.0
Relative permittivity of materials	
FRP tube	2.5
MO block	620.0
Silicone sheds	3.45
Air/N_2	1.0

mm with the height of 700 mm, non-uniformity voltage factor is found to be reduced to within ±17%. To improve non-uniformity voltage factor further, height and diameter of the shield have been increased to 900 mm and 1,400 mm respectively (Fig. 8(b)). The non-uniformity factor is reduced to ±9% with improved grading shield design.

7. Conclusion

The geometrical parameters of the composite insulator clad SA for rated voltage of 420 kV class are estimated in the present paper. To determine these parameters, a generic tool has been developed in ANSYS using the APDL platform with the necessary user interface designed in VB.NET. The numerical model for the MO-stacked composite insulator along with its supporting structure has been generated with appropriate boundary conditions. The integrated structure has been analysed for both static and dynamic considerations as per the standards. In HV substations, composite insulators act as main load-carrying structure. The SA composite insulator transfers dead weights of top connectors, grading shield at the top, MO blocks and aluminium alloy flanges in the axial direction of the FRP tube. For wind and seismic effects of electrical equipment, flexural performance of composite insulator is more important. To study the effect of each (geometric/load) parameter in finalizing the geometric dimensions of the integrated structure, sensitivity analyses have been conducted to compute the effect of various parameters on the structural responses. The cantilever deflection is most sensitive to the thickness variation of flange (FT) followed by insulator tube thickness (OD) and elastic modulus of FRP tube (E-FRP). For reduced cantilever deflections, it

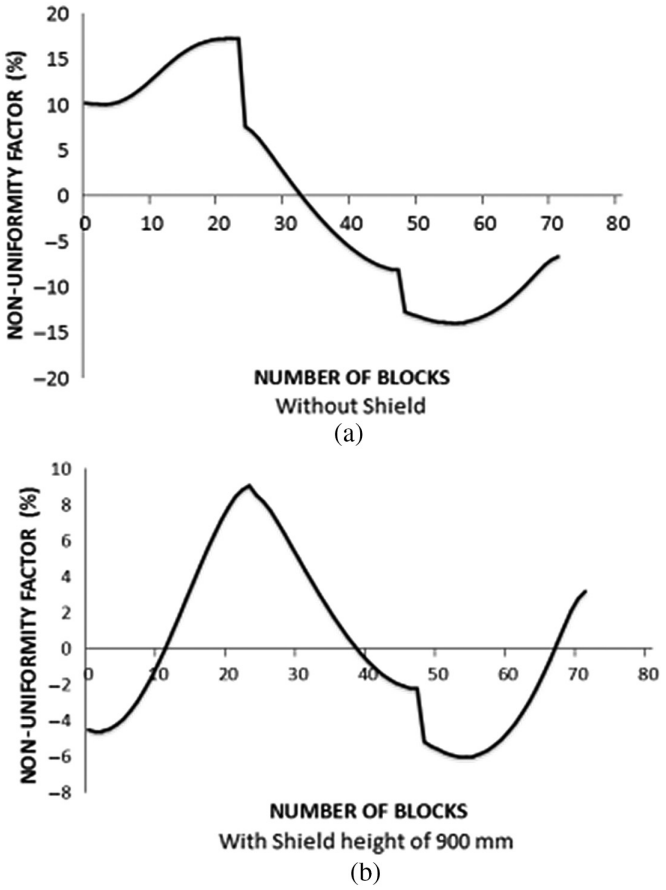

Figure 8. Variation of non-uniformity voltage factor across SA blocks.

may be convenient to select a higher flange thickness rather than opting for superior mechanical properties or higher thickness for insulator tube to limit the cost of the product. E-field analysis on 420 kV AIS SA has been carried out by considering grading shield. Finally, the voltage distribution across SA blocks is estimated by considering HT grading shield optimized through E-field analysis. The non-uniformity voltage factor for 420 kV AIS SA is found to be within ±9%.

References

[1] K.H. Nay, Analysis and design selection of lightning arrester for distribution substation, *World Academy of Science, Engineering and Technology*, *48*, 2008, 174–178.

[2] E. Fujasaki, S. Takhirov, Q. Xie, and K.M. Mosalam, Seismic vulnerability of power supply: Lessons learned from recent earthquakes and future horizons of research, *Proc. 9th International Conference on Structural Dynamics (ICSD), EURODYN 2014*, Portugal.

[3] S. Li, H.H. Tsang, Y. Cheng, and Z. Lu, Considering seismic interaction effects in designing steel supporting structure for surge arrester, *Journal of Constructional Steel Research, 132*, 2017, 151–163.

[4] S. Li, Y. Cheng, Z. Lu, Z. Zhu, and M. Zhong, Seismic performance study of composite insulator assembled in 1000 kV capacitor voltage transformer by quasi-static test and shaking table test", *16th World Conference on Earthquake Engineering (WCEE)*, No. 946, Santiago Chile, 2017.

[5] R.K. Mohammadi, V. Akrami, and F. Nikfar, Dynamic properties of substation support structures, *Journal of Constructional Steel Research, 125*, 2019, 173–178.

[6] IEEE-693, *Recommended Practice for Seismic Design of Substations* (New York: IEEE, 2005).

[7] M.A. Moustafa and K.M. Mosalam, Structural performance of porcelain and polymer post insulators in high voltage electrical switches, *Journal of Performance of Constructed Facilities*, *30*(5), 2016.

[8] A.S. Whittaker, G.L. Fenves, and A.S.J. Gilani, Seismic evaluation and analysis of high voltage substation disconnect switches, *Engineering Structures*, *29*(12), 2007, 3538–3549.

[9] S. Li, H.H. Tsang, Y. Cheng, and Z. Lu, Effects of sheds & cemented joints on seismic modelling of cylindrical porcelain electrical equipment in substations, *Earthquakes & Structures*, *12*(1), 2017, 55–65.

[10] H. Chang, X. Qiang, Y. Zhenyu, and X. Sontago, Seismic performance evaluation and improvement of ultra-high voltage wall bushing-valve hall system, *Journal of Constructional Steel Research*, *154*, 2019, 123–133.

[11] N. Ullah, S.M. Ali, R. Shahzad, and F. Khan, Seismic qualification and time history shake table testing of high voltage surge arrester under seismic qualification level moderate, *Cogent Engineering*, *5*, 2018.

[12] ANSYS Elements Reference, Release 17.0.

[13] S. Li, H.H. Tsang, Y. Cheng, and Z. Lu, Seismic testing and modelling of cylindrical electrical equipment with GFRP composite insulators, *Composite Structures*, *194*, 2018, 454–567.

[14] R.K. Mohammadi, F. Nikfar, and V. Akrami, Estimation of required slack for conductors connecting substation equipment subjected to earthquake, IEEE Transactions *on* Power Delivery, *27*(2), 2012, 709–717.

[15] IS 875 (Part 3): *2015 Code of Practice- Design Loads for Buildings and Structures*, BIS, New Delhi.

[16] IS 1893 (Part 4): *2015 Criteria for Earthquake Resistant Design of Structures – Industrial Structures Including Stack-Like Structures*, Bureau of Indian Standards, New Delhi.

[17] V.S. Brito, G.R.S. Lira, E.G. Costa, and M.J.A. Maia, A wide-range model for metal-oxide surge arrester, IEEE Transactions on Power Delivery, *33*(1), 2018, 102–109.

Biographies

Konthedath M.M. Muneer completed his M.S. by Research in 2010 from Machine Design Section, Department of Mechanical Engineering, Indian Institute of Technology (IITM), Madras. He is associated with Bharat Heavy Electricals Limited (BHEL), Corporate R&D, since 2010. His areas of interest are structural design and development of design automation tools for supporting systems of power plant equipment.

Neelam Tiwari completed her B.Tech. degree in Electrical Engineering from NIT Bhopal, India, in 2005. She is associated with Bharat Heavy Electricals Limited (BHEL), since 2005 and presently, she is a Manager at BHEL R&D. Her research areas of interest are design and development of Gas Insulated Substations, Hybrid gas insulated switchgear, compact bus ducts and Surge Arresters.

Supak Pore completed his M.E in 2005 from Department of Applied Mechanics, Bengal Engineering and Science University, Shibpur, Howrah. He is associated with Bharat Heavy Electricals Limited (BHEL), Corporate R&D since 2007 and presently, he is a Manager in Design Analysis Group. He is specialized in structural mechanics and design of power plant equipment.

Manish C. Gupta completed his Master of Science in Engineering in 2012 from Department of Mechanical Engineering, Indian Institute of Science (IISc), Bangalore. He is associated with Bharat Heavy Electricals Limited (BHEL), since 2001 and presently, he is the Deputy General Manager (DGM), in-charge of Design Analysis Group, Corporate R&D BHEL. He is specialized in structural mechanics and design of power plant equipment.

Mandava M. Rao completed his Master of Science in Engineering degree in 1996 and Ph.D. degree in 2006 from High Voltage Department of Electrical Engineering division, Indian Institute of Science, Bangalore. He is associated with Bharat Heavy Electricals Limited, R&D, since 1996 and presently, he is the Sr. Dy. General Manager, in-charge of Gas Insulated Power Equipment and Switchgear Group, Corporate R&D, BHEL. His research areas of interest are design and development of gas insulated substations, hybrid gas insulated switchgear, circuit breakers, gas insulated transmission lines and surge arresters.